(Not for publication) Online Appendix to
"The Macroeconomic Consequences of Natural Rate Shocks"

Stephanie Schmitt-Grohé and Martín Uribe

forthcoming, Review of Economics and Statistics
December 10, 2024

A The Empirical Model in State Space Form and Impulse Response Functions

In this section of the online appendix we show how to cast the empirical model described by equations (3)–(7) in state space form and how to compute impulse response functions. For expositional purposes the derivation omits intercepts and deterministic trends. Let

$$\hat{Y}_t \equiv \begin{bmatrix} \hat{y}_t & \hat{\pi}_t & \hat{i}_t \end{bmatrix}'$$

$$u_t \equiv \begin{bmatrix} \Delta X_t^m & z_t^m & \Delta X_t & z_t & \Delta X_t^r \end{bmatrix}'$$

$$\epsilon_t \equiv \begin{bmatrix} \epsilon_t^{X^m} & \epsilon_t^{z^m} & \epsilon_t^X & \epsilon_t^z & \epsilon_t^{X^r} \end{bmatrix}'.$$

Equations (3) and (4) can then be written, respectively, as

$$\widehat{Y}_t = B\widehat{Y}_{t-1} + Cu_t \tag{A1}$$

$$u_{t+1} = \rho u_t + \psi \epsilon_{t+1}. \tag{A2}$$

Let

$$\xi_t \equiv \begin{bmatrix} \widehat{Y}_{t-1} & u_t \end{bmatrix}'$$

and write (A1) and (A2) as

$$\xi_{t+1} = F\xi_t + P\epsilon_{t+1}$$

with

$$F = \begin{bmatrix} B & C \\ \emptyset_{n_u \times n_y} & \rho \end{bmatrix} \quad \text{and} \quad P = \begin{bmatrix} \emptyset_{n_y \times n_u} \\ \psi \end{bmatrix},$$

where n_u is the length of the vector u_t and n_y is the length of the vector $\widehat{Y}_t$. Let

$$o_t \equiv \begin{bmatrix} \Delta y_t & \Delta \pi_t & \Delta i_t \end{bmatrix}' \quad \text{and} \quad \mu_t \equiv \begin{bmatrix} \mu_t^y & \mu_t^\pi & \mu_t^i \end{bmatrix}'.$$

Write equations (5), (6), and (7) as

$$o_t = H_1 \widehat{Y}_t + H_2 \widehat{Y}_{t-1} + H_3 u_t + \mu_t \tag{A3}$$

where

$$H_1 = \begin{bmatrix} 1 & 0 & 0 \\ 0 & 1 & 0 \\ 0 & 0 & 1 \end{bmatrix}; \quad H_2 = \begin{bmatrix} -1 & 0 & 0 \\ 0 & -1 & 0 \\ 0 & 0 & -1 \end{bmatrix}; \quad \text{and} \quad H_3 = \begin{bmatrix} 0 & 0 & 1 & 0 & \delta \\ 1 & 0 & 0 & 0 & 0 \\ 1 & 0 & 0 & 0 & 1 \end{bmatrix}.$$

Use (A1) to eliminate $\widehat{Y}_t$ from (A3). This yields

$$o_t = H' \xi_t + \mu_t; \quad \text{with } H' \equiv \begin{bmatrix} H_1 B + H_2 & H_1 C + H_3 \end{bmatrix}.$$

In summary, the state space model consists of the following state and observation equations

$$\xi_{t+1} = F \xi_t + P \epsilon_{t+1} \tag{A4}$$

$$o_t = H' \xi_t + \mu_t, \tag{A5}$$

where ξ_t denotes the vector of latent state variables and o_t denotes the vector of observables.

The impulse response in period t of ξ_t to an innovation in the vector ϵ_t in period 0, is equal to $F^t P \epsilon_0$. The impulse response in period t of o_t to an innovation in period 0 is equal to

$H'F^tP\epsilon_0$. The period-t impulse response of y_t, π_t, and i_t to an ϵ_0 shock is equal to the sum of the impulse responses of the respective changes between periods 0 and t given by the impulse responses of o_t. Finally, the impulse response of the real rate, defined as, $i_t - E_t\pi_{t+1}$, to an ϵ_t shock in period 0, is equal to the period-t response of i_t minus the period-t+1 response of π_t.

B Further Information on Estimation and Robustness

B.1 Postwar Sample for Quarterly and Annual Data

One potential advantage of working with long data, that is, with data that starts in 1900, is that one can better identify the permanent component of a time series. But working with long data also comes with potential drawbacks. One drawback, as discussed in the body of the paper in section 5.2, is that pre-postwar data is noisier than postwar data. Another drawback is that pre-postwar data, even after controlling for larger measurement error, is more volatile than postwar data. This could be due to larger fundamental shocks hitting the economy or to differences in the effectiveness of stabilization policy. It is therefore of interest to investigate to what extend the results obtained with long data continue to hold when one restricts attention to the postwar sample. An additional advantage of using postwar data is that quarterly data is available for the postwar period, whereas no such data exists for the prewar period. Accordingly, in this section of the online appendix we estimate the model over the sample period 1960 to 2023 using both annual and quarterly data. We begin by presenting the specification of the quarterly model and the assumed prior distributions of its estimated parameters.

Table B1: Prior Distributions: Quarterly Model

Parameter	Distribution	Mean	Std. Dev.
Diagonal elements of B_1	Normal	0.95	0.5
Off diagonal elements of B_1	Normal	0	0.25
Elements of B_2, B_3, B_4	Normal	0	0.25
C_{21}, C_{31}	Normal	-1	1
All other estimated elements of C	Normal	0	1
ρ_{ii}, $i = 1, 2, 3, 5$	Beta	0.3	0.2
ρ_{44}	Beta	0.7	0.2
Diagonal elements of ψ	Gamma	1	1
δ	Normal	0	5
Diagonal elements of R	Uniform	$\frac{\text{var}(o_t)}{10\times 2}$	$\frac{\text{var}(o_t)}{10\times\sqrt{12}}$
Estimated element of A	Normal	$E(\Delta y_t)$	$\sqrt{\frac{\text{var}(\Delta y_t)}{T}}$

Notes. The variable T denotes the sample length. The vector o_t contains the observables, $o_t = [\Delta y_t \ \Delta\pi_t \ \Delta i_t]'$. The vector A denotes the mean of the vector of observables, $A = E(o_t)$.

B.1.1 Specification of the Quarterly Model

When the model is estimated on quarterly data, the cyclical components of the endogenous variables are assumed to follow the fourth-order autoregressive process

$$\begin{bmatrix} \hat{y}_t \\ \hat{\pi}_t \\ \hat{i}_t \end{bmatrix} = \sum_{j=1}^{4} B_j \begin{bmatrix} \hat{y}_{t-j} \\ \hat{\pi}_{t-j} \\ \hat{i}_{t-j} \end{bmatrix} + C \begin{bmatrix} \Delta X_t^m \\ z_t^m \\ \Delta X_t \\ z_t \\ \Delta X_t^r \end{bmatrix}. \tag{B1}$$

Equation (B1) replaces equation (3) of the annual model presented in the body of the paper. All other model equations are unchanged.

The data sources for quarterly observations on real GDP per capita, inflation, and the short-term nominal interest rate are the same as those given in section 2.3 of the paper for the updates of the annual data starting in 2017.

Table B1 presents information on the assumed prior distributions of the parameters of

Figure B1: The Natural Rate of Interest: 1960–2023

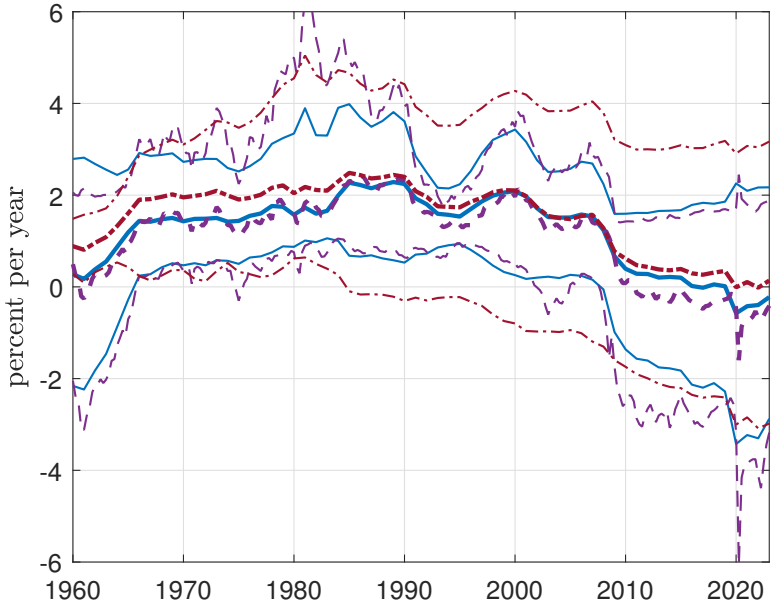

Notes. The figure plots the posterior median of X_t^r (bold lines) and the 2.5th and 97.5th posterior percentile of X_t^r (fine lines) based on the estimation from three different data sets: annual data from 1960 to 2023 (solid lines); quarterly data from 1960Q1 to 2023Q4 (broken lines); and annual data from 1900 to 2023 (dash dotted line), which is repeated from Figure 1 of the body of the paper. The variable X_t^r is computed by two-sided Kalman smoothing. It is normalized by adding a constant to match the observed sample mean of $i_t - \pi_{t+1}$. The posterior medians and posterior percentiles are computed using 100,000 randomly picked draws from the respective MCMC chains of length 50 million.

the quarterly model.

B.1.2 Natural Rate Supercycles: Postwar Sample

Figure B1 presents the estimated path of X_t^r when the model is estimated either on annual (solid lines) or quarterly (broken lines) postwar data. For comparison it also repeats the estimated path of X_t^r from the full sample estimation (dash dotted lines) shown in Figure 1 of the body of the paper. The posterior medians from the quarterly and annual postwar sample are fairly close to each other and also to the estimate based on the full sample. The figure supports the narrative that the natural rate exhibits supercycles, with the most recent upswing beginning before the 1960s, peaking in the mid-1980s, and then entering a downward phase. It also continues to be the case that the fall in the natural rate is estimated

Figure B2: The Natural Rate of Interest: Comparison with the FRBNY-LW Estimate

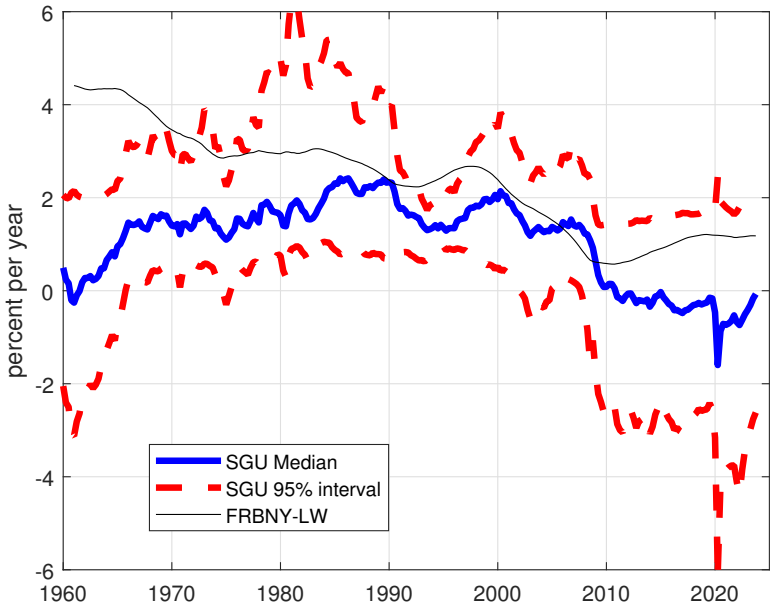

Notes. The lines labeled SGU reproduce the estimate of X_t^r on quarterly data from 1960Q1 to 2023Q4 displayed in Figure B1. The line labeled FRBNY-LW corresponds to the natural rate estimate of the Laubach-Williams model published by the Federal Reserve Bank of New York (2024).

to have been particularly pronounced during the financial crisis of 2008.

The results from the estimation of the model on postwar data are broadly in line with existing related estimates of the natural rate that use postwar U.S. data, such as those available on the website of the Federal Reserve Bank of New York (2024), which are based on the work of Laubach and Williams (2003). Figure B2 displays the estimate obtained here and that of the Federal Reserve Bank of New York. The latter lies inside the credible bands of the quarterly estimate performed here for most of the sample period. Both estimates indicate that the natural rate displayed a declining path since the mid 1980s. However, the present estimate suggests that the natural rate increased from 1960 to the mid 1980s—consistent with the supercycle estimated with data since 1900 and with the estimates in Del Negro et al. (2017, 2019)—whereas the Federal Reserve Bank of New York estimate displays a declining trajectory since 1960.

Figure B3: Estimation Sample 1960 to 2023: Prior and Posterior Densities of δ

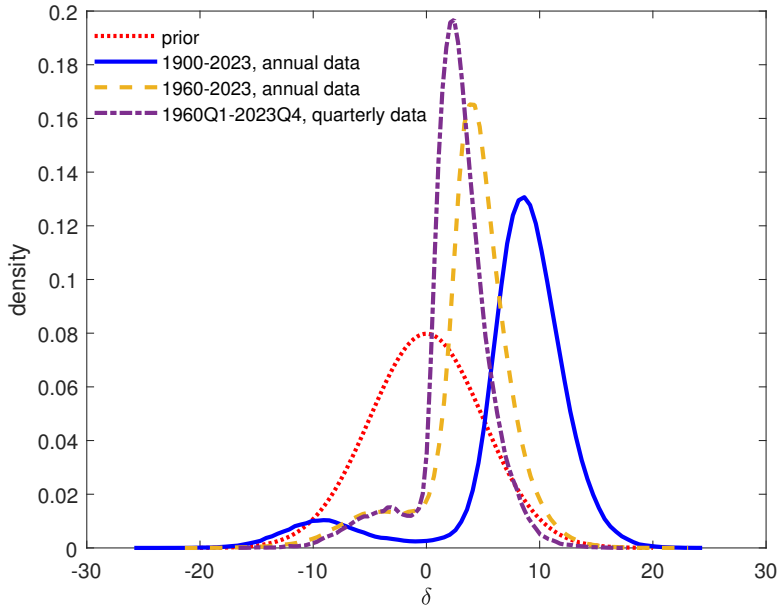

Notes. The parameter δ measures the effect of a change in the natural rate of interest, X_t^r, on the trend level of output. A positive value of δ means that a decline in the natural rate of interest (a fall in X_t^r) lowers the trend level of output.

B.1.3 Effects of Natural Rate Shocks on the Trend of Output: Postwar Sample

Figure B3 displays the prior and posterior densities of the parameter δ measuring the long run impact of a change in the natural rate on the trend level of output. Estimates from postwar data with annual frequency are shown with a broken line and estimates from postwar data with quarterly frequency are shown with a dash-dotted line. For comparison, the figure also reproduces from Figure 2 of the body of the paper the prior density (dotted line) and the posterior density when the model is estimated on the long annual data (solid line).

The figure shows that holding the frequency of the observations constant, the posterior mean of δ is smaller when the model is estimated on the postwar sample compared to the full sample. Specifically, the posterior mean of δ falls from 7.5 in the 1900-to-2023 sample to 3.7 in the 1960-to-2023 sample. Furthermore, holding the sample period, 1960 to 2023, constant, the posterior mean of δ is smaller when the model is estimated using quarterly data instead of annual data. In this case, the posterior mean falls from 3.7 to 2.6.

Table B2: Prior and Posterior First and Second Moments of ρ_{55} and ψ_{55}

	Mean(ρ_{55})	Std(ρ_{55})	Mean(ψ_{55})	Std(ψ_{55})
Prior	0.30	0.20	1.00	1.00
Posterior, 1900-2023	0.31	0.12	0.45	0.16
Posterior, 1960Q1-2023Q4	0.14	0.13	0.23	0.14

Note. Posterior moments are computed using 100,000 randomly picked draws from an MCMC chain of length 50 million.

At the same time, the posterior likelihood that the parameter δ is positive is about the same across the three data sets, namely, 91 percent in the annual data starting in 1900, 88 percent in the annual data starting in 1960, and 89 percent in the quarterly data starting in 1960Q1. These results suggest that the finding that a decrease in the natural rate lowers the trend path of output is robust to cutting the sample size in half by starting it in 1960 instead of 1900 and changing the data frequency from annual to quarterly.

B.2 Identification of the Parameters Governing the Evolution of $\boldsymbol{X_t^r}$

The present paper investigates the effects that innovations to the natural rate have on output and inflation. So it is natural to ask whether the parameters governing the evolution of X_t^r are well identified. One way of approaching this question is to ask if their posterior distributions differ meaningfully from their assumed prior distributions. Accordingly, here we present a comparison of the prior and posterior distributions of these parameters. We will do this for the estimation of the model on annual data from 1900 to 2023 and for the estimation on quarterly postwar data. The inclusion of the quarterly dataset is motivated by facilitating comparison with existing related work that argues that there is little difference between prior and posterior densities of the parameters governing the standard deviation of the innovations to the natural rate, such as Kiley (2020), which uses postwar quarterly data.

Figure B4: Prior and Posterior Densities of ρ_{55} and ψ_{55}

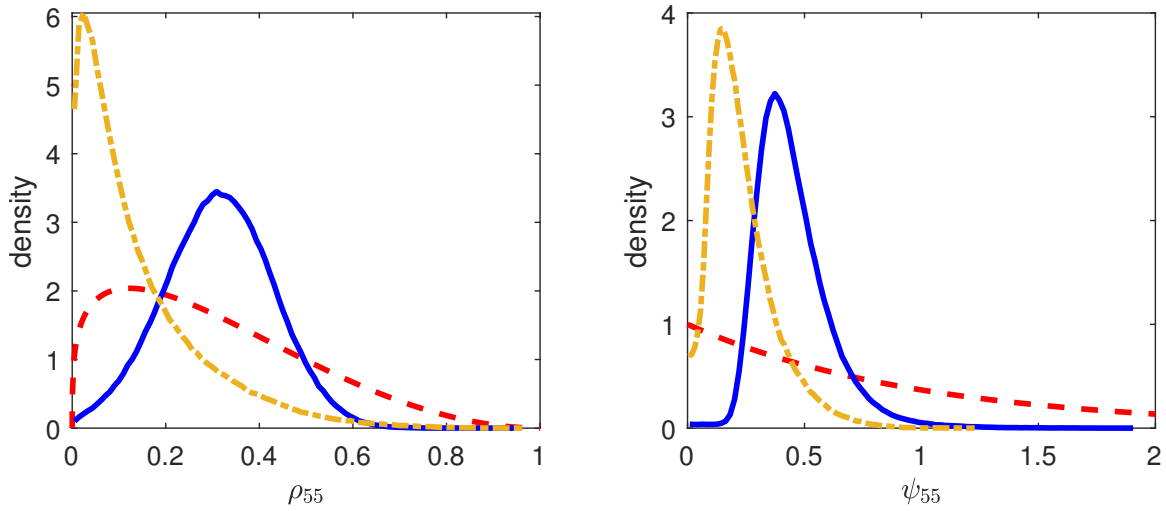

Notes. The law of motion of ΔX_t^r is $\Delta X_t^r = \rho_{55}\Delta X_{t-1}^r + \psi_{55}\epsilon_t^{X^r}$, where $\epsilon_t^{X^r}$ is an i.i.d. disturbance distributed $\mathcal{N}(0,1)$. Prior densities are shown with broken lines. Posterior densities are shown with solid lines (estimation on annual 1900–2023 data) or dash-dotted lines (estimation on quarterly 1960Q1 to 2023Q4 data).

Recall from equation (4) that X_t^r is assumed to evolve over time as

$$\Delta X_{t+1}^r = \rho_{55}\Delta X_t^r + \psi_{55}\epsilon_{t+1}^{X^r},$$

where $\epsilon_{t+1}^{X^r}$ is an i.i.d. disturbance distributed $\mathcal{N}(0,1)$. The parameter ρ_{55} is assumed to have a Beta prior distribution and the parameter ψ_{55} a Gamma distribution. Table B2 presents the prior and posterior means and standard deviations. The table shows that there are large differences between the prior and posterior moments with the exception of ρ_{55} for which in the annual estimation on long data the prior and posterior means are basically equal.

Large differences between the prior and the posterior are also evident when comparing the prior and posterior densities of ρ_{55} and ψ_{55}. Figure B4 shows that these densities are quite distinct. Notably, although the posterior mean of ρ_{55} estimated for the period 1900 to 2023 is similar to its prior mean, its posterior density differs significantly from its prior density.

Taken together, the results reported in Table B2 and Figure B4 suggest that the data

contains information about the parameters governing the exogenous process for the natural rate of interest. These findings differ from those reported in Kiley (2020) who concludes, working with quarterly postwar data, that there is little information to identify those parameters. Kiley's empirical model differs in a number of aspects from the one presented here. A potentially important one is that in the present framework, the natural interest rate and the trend level of output are allowed to share a permanent component, whereas in the model of Kiley they are not. In other words, in terms of the notation of the present model, Kiley imposes that δ is equal to zero. This is a key parameter of our framework as it governs the effects of changes in the natural rate on economic activity. A central result of the present paper is that the data strongly prefers a large positive value of δ. A further difference is that the model of Kiley, like the model of Laubach and Williams (2003), assumes that the growth rate of output has a unit root, whereas the model of the present paper estimates that the growth rate of output is stationary.

B.3 The Cyclical Component of Output, $\hat{y}_t$

One of the latent variables of the model is the cyclical component of output, denoted $\hat{y}_t \equiv y_t - (X_t + \delta X_t^r)$. Some studies in the related literature (see, for example, Zaman 2024, and the references cited therein) argue that simple models of the natural rate using information on just output, the nominal interest rate, and inflation, as we do, may imply estimates of the cyclical component of output that are at odds with conventional views on its properties. For this reason, it is of interest to present the implications of our model regarding the cyclical component of output.

Figure B5 shows, with a solid line, the posterior median of $\hat{y}_t$ and, with broken lines, the 95-percent posterior interval based on a random sample of 100,000 draws from an MCMC chain of length 50 million. The figure also indicates NBER recession dates with shaded areas. The figure shows that, in general, the implied fluctuations in $\hat{y}_t$ are fairly transitory and that declines in $\hat{y}_t$ align with NBER recessions.

Figure B5: The Cyclical Component of Output, $\hat{y}_t$, 1900-2023

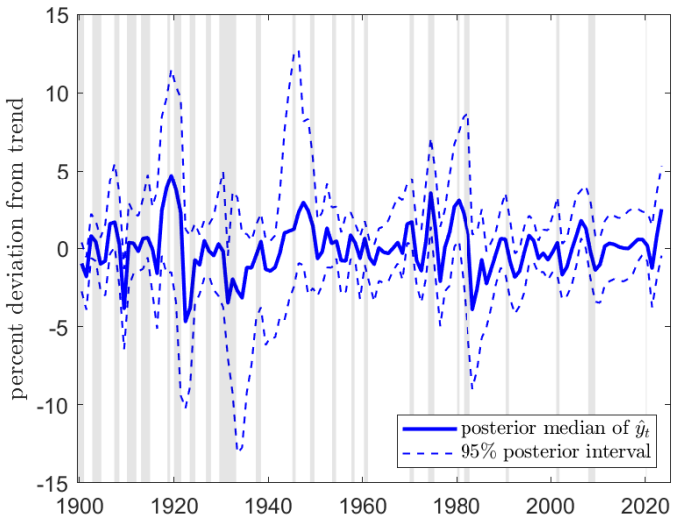

Notes. The variable $\hat{y}_t$ is computed by two-sided Kalman smoothing. The solid line is the posterior median of $\hat{y}_t$ and the broken lines indicate the 2.5th and 97.5th posterior percentile of $\hat{y}_t$, respectively. These statistics are computed using 100,000 randomly picked draws from an MCMC chain of length 50 million. Shaded areas indicate NBER recession dates.

Zaman (2024) and the papers cited therein work with postwar data, while our estimates are based on data since 1900. Thus, one way to relate our findings to those studies is to compare the cyclical component of Hodrick-Prescott (HP) filtered output and $\hat{y}_t$ for the postwar period, 1960–2023. Specifically, using an HP smoothing parameter of 6.25 as recommended for annual data by Ravn and Uhlig (2002), the standard deviation of HP filtered output is 1.35, and the first-order autocorrelation is 0.22. If one instead uses an HP smoothing parameter of 100, which is also widely used in the business-cycle literature, then, as expected, both moments are higher; the standard deviation of HP filtered output is 1.92, and the serial correlation is 0.51. This suggests that a reasonable range in the postwar period for the standard deviation of $\hat{y}_t$ is 1.35 to 1.92, and a reasonable range for the serial correlation is 0.22 to 0.51. The posterior median of $\hat{y}_t$ has, over the period 1960–2023, a standard deviation of 1.34 and a serial correlation of 0.47, placing it in close vicinity to this reasonable range. We regard these results as supporting the view that the business cycle properties of the cyclical

component of output implied by our model are not necessarily at odds with conventional wisdom.

B.4 Alternative Priors for ψ_{55}

In this section we consider the effects of lowering the mean and standard deviation of the prior distribution for the parameter ψ_{55}, governing the standard deviation of the innovation to changes in the natural rate of interest, ΔX_t^r, see equation (4), on the marginal data density. Specifically, we consider 3 alternatives. In all three the prior distribution is Gamma. In the first the mean and standard deviation are half as large as in the baseline case (Alternative 1), in the second they are one fourth as large as in the baseline case (Alternative 2), and in the third they are 1/100 as large as in the baseline case (Alternative 3). All other aspects of the model are unchanged. After reestimating the model under these three alternative prior specifications, we compute the marginal likelihood of the data using the modified harmonic mean estimator of Geweke (1999). Table B3 presents the results and shows that given a truncation parameter, the marginal likelihood of the data is highest under the baseline prior parameterization.

B.5 Impulse Responses to Other Permanent Shocks

Figure B6 displays the impulse response functions to the permanent shocks X_t^m and X_t.

The permanent monetary shock, X_t^m, produces neo-Fisherian dynamics, in line with the results in Uribe (2017, 2022). That is, a permanent increase in the nominal interest rate generates inflation not only in the long run (the Fisher effect), but also in the short run (the neo-Fisher effect). This shock is also expansionary in the short run, in line with the findings in the related literature (Uribe, 2017, 2022; Azevedo, Ritto, and Teles, 2022). The novel insight of Figure B6 is that the neo-Fisher effect is present not only in postwar data, as established in the papers just cited, but also in data starting as early as 1900.

The permanent output trend shock, X_t, is expansionary both in the short and long

Table B3: Marginal Data Densities for Alternative Prior Means and Standard Deviations of ψ_{55}

Truncation parameter	Baseline	Alternative 1	Alternative 2	Alternative 3
0.1	-922.42	-924.70	-922.64	-928.16
0.2	-922.42	-924.04	-923.43	-927.58
0.3	-922.14	-923.66	-923.11	-927.25
0.4	-921.97	-923.40	-924.44	-926.98
0.5	-921.85	-923.21	-924.22	-926.78
0.6	-921.78	-923.04	-924.05	-926.63
0.7	-921.65	-922.89	-923.91	-926.50
0.8	-921.56	-922.77	-923.78	-926.39
0.9	-921.45	-922.67	-923.66	-926.27

Notes. The table reports the natural logarithm of the marginal data density when the parameter ψ_{55} is assumed to have a Gamma prior distribution with a mean and standard deviation equal to 1 (Baseline), 0.5 (Alternative 1), 0.25 (Alternative 2), or 0.01 (Alternative 3). The marginal data density is computed using 1 million random draws from an MCMC chain of length 50 million.

Figure B6: Impulse Responses to X_t^m and X_t

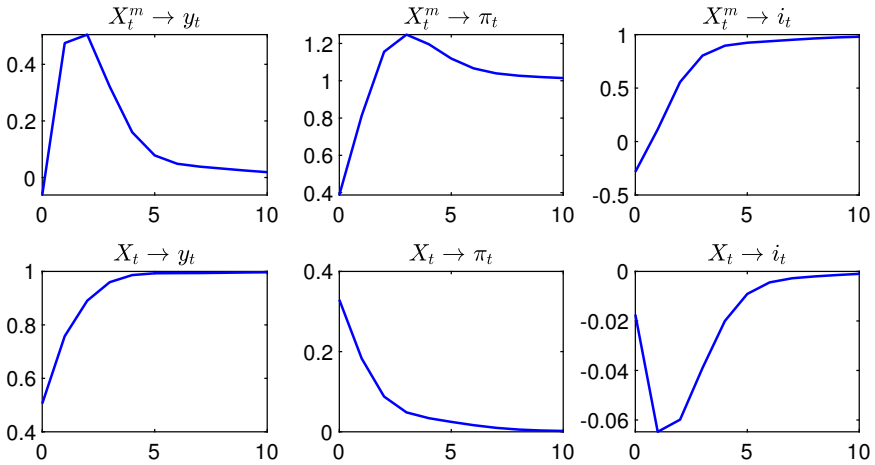

Notes. Impulse responses are posterior means computed from 100,000 random draws from an MCMC chain of length 50 million. The innovation to X_t^m is set so that the nominal interest rate increases by one annual percentage point in the long run. The innovation to X_t is set so that output increases by 1 percent in the long run. The unit on the horizontal axes is years after the shocks. The response of output is measured in percent deviation from the pre-shock level. The responses of inflation and the interest rate are in deviations from the pre-shock level in percentage points per year.

runs. Interestingly, an increase in X_t is inflationary in the short run. This may capture the fact that, since ΔX_t is positively serially correlated, when X_t increases, productivity is expected to be higher in the future than on impact, which can cause a short-run expansion in investment and consumption larger than the short-run expansion in production capacity. At the same time, the estimated response of the nominal rate is muted.

B.6 Forecast Error Variance Decompositions

How important is the natural rate shock? To address this question, we conduct a forecast error variance decomposition of the levels of output per capita, y_t, inflation, π_t, and the nominal interest rate, i_t, for the estimated model for three cases: when the model is estimated on annual 1900 to 2023 data, on quarterly 1961Q1 to 2023Q4 data, and on annual 1960 to 2023 data. The results are displayed in Figures B7, B8, and B9, respectively. For all three data samples, the identified natural rate shock X_t^r is macroeconomically relevant.

The bottom left panel of Figure B7 shows that in the 1900 to 2023 annual sample, on average, the natural rate shock explains more than 80 percent of the forecast error variance of output at horizons of 1 to 10 years. The 95-percent posterior interval for the forecast error variance decomposition of y_t (not shown) is relatively wide, but the 2.5th posterior percentile remains above 20 percent across all forecasting horizons, supporting the interpretation that the X_t^r shock is economically significant. The bottom left panels of Figures B8 and B9 show that the natural rate shock explains more than 50 percent of the forecast error variance of output at horizons of 1 to 10 years on average when the model is estimated on quarterly or annual data from 1960 to 2023. While 50 percent is lower than the 80 percent found when the model is estimated on long data, it continues to be the case that the X_t^r shock is estimated to be the most important driver of output.

The figures also address the question of what factors explain inflation variations. The answer to this question turns out to depend on the estimation sample. As is well known, real variables are significantly more volatile in the first half of the 20th century. This is reflected

in a larger role of real disturbances in explaining movements in inflation when the model is estimated using data starting in 1900 than when it is estimated using data starting in 1960. In the postwar era, monetary shocks, and in particular the permanent monetary shock X_t^m, play a more dominant role, consistent with the results in Uribe (2017, 2022). Figure B7 shows that for the estimation on data from 1900 to 2023, at a forecasting horizon of 5 years, for example, the forecast error variance of inflation is explained to a large extend by 3 shocks: The permanent monetary shock, X_t^m, explains 22 percent; the permanent technology shock, X_t, 35 percent, and the transitory real shock z_t 38 percent. Estimating the model over the period 1960 to 2023 at annual frequency yields a forecast error variance decomposition of inflation at a 5-year horizon in which X_t^m explains 61 percent, X_t 15 percent, and z_t 19 percent (see Figure B9).

Figure B7: Forecast Error Variance Decomposition: Annual Data 1900 to 2023

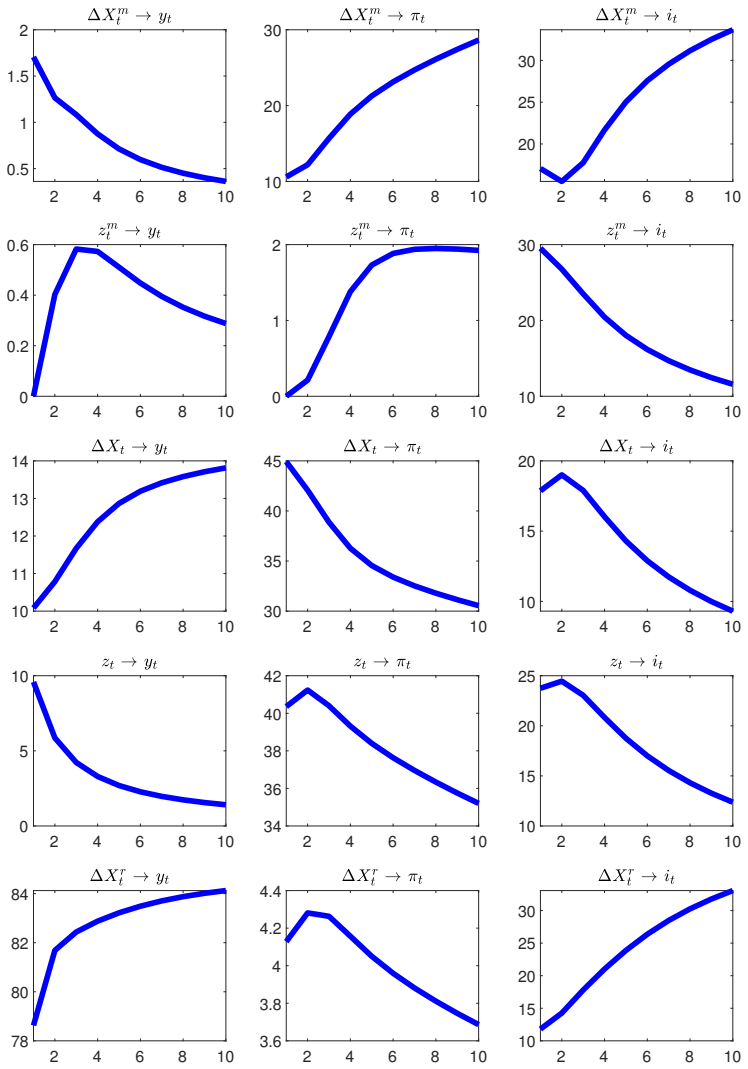

Notes.Vertical axes measure shares in percent, and horizontal axes measure forecast horizons in years. Forecast error variance shares are means from 100 thousand draws from the posterior distribution of the forecast error variance shares.

Figure B8: Forecast Error Variance Decomposition: Quarterly Data 1960Q1 to 2023Q4

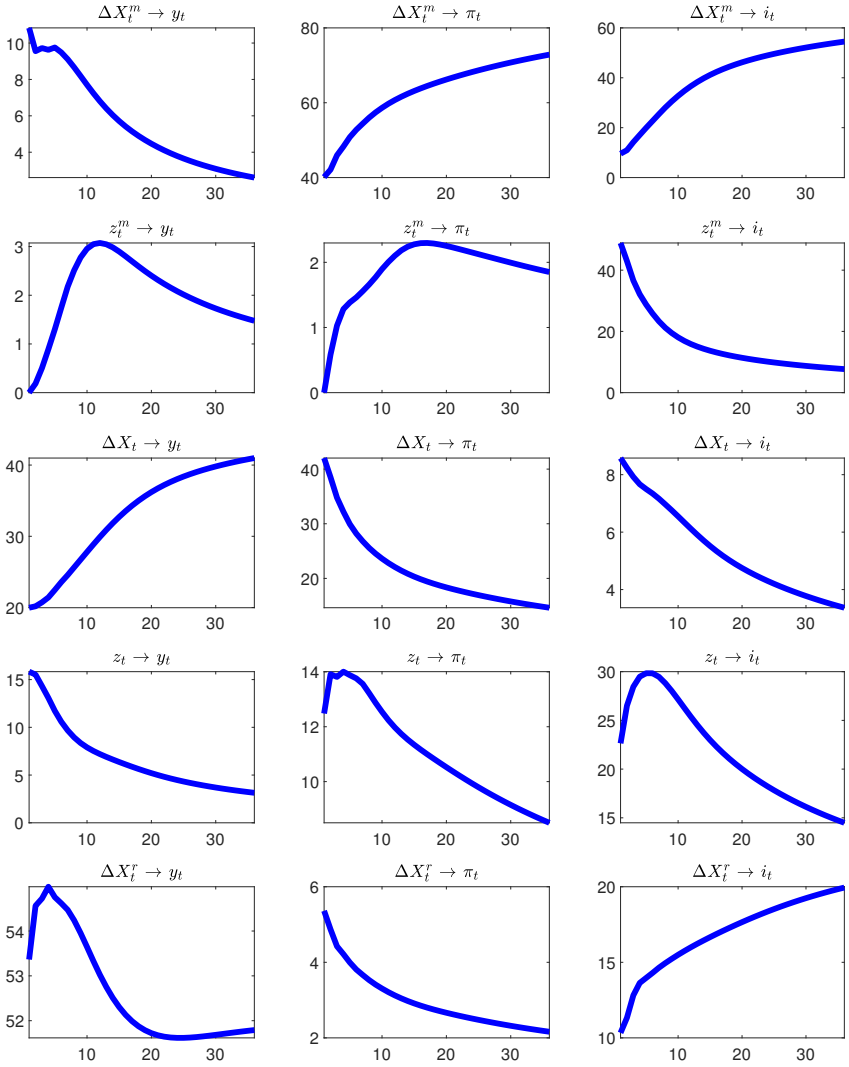

Notes.Vertical axes measure shares in percent, and horizontal axes measure forecast horizons in quarters. Forecast error variance shares are means from 100 thousand draws from the posterior distribution of the forecast error variance shares.

Figure B9: Forecast Error Variance Decomposition: Annual Data 1960 to 2023

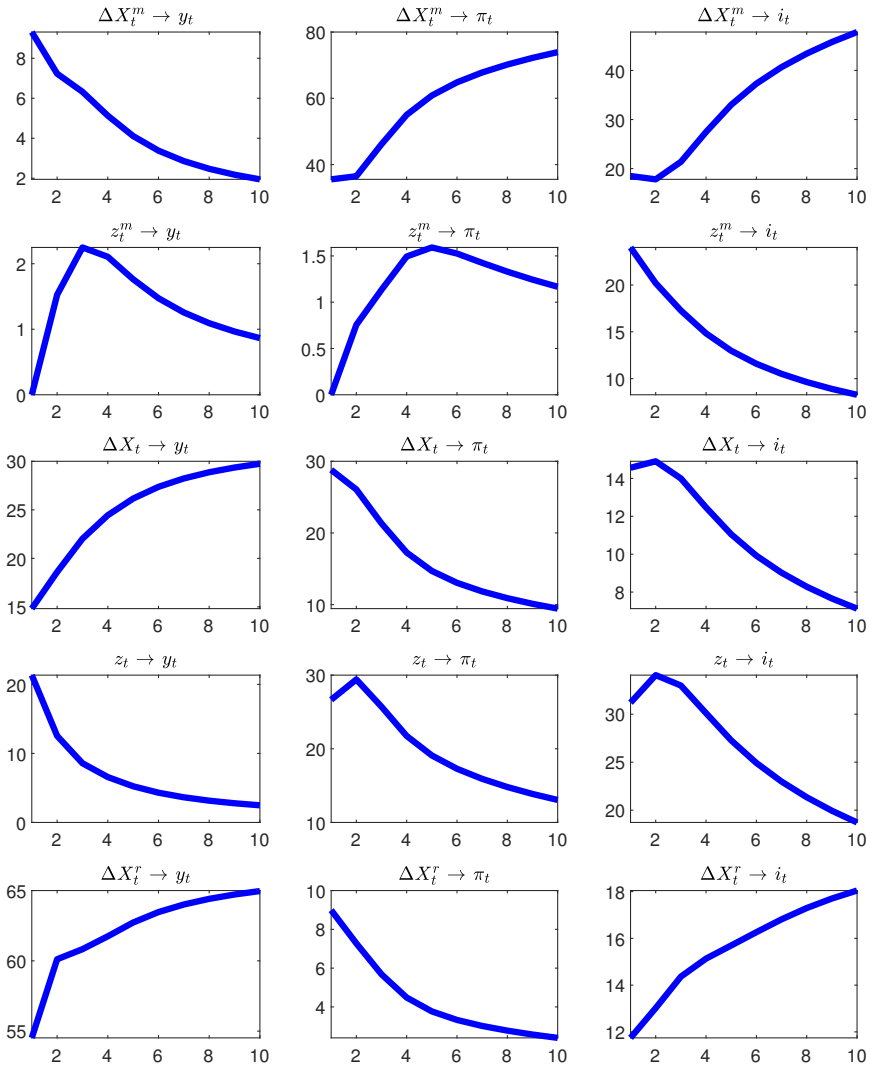

Notes.Vertical axes measure shares in percent, and horizontal axes measure forecast horizons in years. Forecast error variance shares are means from 100 thousand draws from the posterior distribution of the forecast error variance shares.